Modeling an optical properties of plant epiticular wax

E.R. Bukhanov[1], Y.L. Gurevich[2], D.A. Shabanov[1]

[1]Kirensky Institute of Physics Federal Research Center Krasnoyarsk Science Center of the Siberian Branch of the RAS, Akademgorodok street 50/38, Krasnoyarsk, Russia, 660036
[2]Federal Research Center Krasnoyarsk Science Center of the Siberian Branch of the RAS, Akademgorodok street 50, Krasnoyarsk, Russia, 660036

Abstract. For the first time optical features of chemically-pure samples of the wax contained in wheat leaves and blue spruce needles have been studied. As part of the study, anisotropy of their structures has been discovered. An elementary unit of the long-period structure is a nanotube sized up to 6 mkm in length with a diameter of approximately 150 nanometres. Our calculations made it possible to explain the characteristic features that affect photosynthetic efficiency in transmission and fluorescence spectra.

1. Introduction

A wax-coated plant cuticle provides a multitasking interface between a plant and the environment. These waxes are located on the surface of plants and called epicuticular wax.

According to [1-6], the cuticle protects plant cells from external influence, water loss, chemicals, and, what is more, affects optical characteristics of light penetrating the photosynthesis reaction center. Surprisingly, plants waxes have similar structures and form a conglomerate of various long-period carbohydrates, aldehydes, acids and alcohols. The chain length is greater than the length of twenty cc-bonds. Their quantitative ratios as well as their morphology vary in different species of plants. Less common components of epicuticular waxes are flavonoids. The most interesting fact is that wax structure has a quite arranged structure [7-12].

Self-formation of waxes was studied in [13-17]. The research showed the role of substrates and temperature. In particular, the orientation of the axes of crystals grown on non-polar substrates differs from the orientation of self-organized crystals on polar substrates. The effect of chirality due to a spiral twist was revealed in these structures [18-20].

Therefore, an incident ray of light falling on a leaf takes on chiral properties on its waxy structure. In this case, diffraction occurs not at different boundaries of materials with different refractive indices but on a smooth gradient caused by rotation of the optical axis. Wave impedance, amplitudes ratio and phases of the electric and magnetic fields remain constant throughout the structure.

The ability to provide periodicity using homogeneous materials provides substantial saving and for this reason is spread widely in wildlife.

The coloration of plants can be caused by chemical pigments or diffraction on a long-period structure. In the latter case, a change in the spatial period leads to a change in color. Non-

pigmented structural colouration has an irisation effect, which means that iridescent colour changes with changing of the view angle. For instance, young Danaea nadosa leaves form chiral cellulose structures with a pitch of approximately 320 nm, which, with a refractive index of 1.5, gives a blue-green reflection in water [18–20]. The helicoidal structure reflects only one of the two circular polarizations of the light wave and does not exceed half of the non-polarized light. To fully reflect the non-polarized light, alternating left and right fixed helicoidal structures or long-period layered media may be used. In wildlife, these layers most often consist of organic substances such as fatty acids and air. The paper [13,21-23] revealed this kind of structure in the wax of blue spruce. Constructive interference that repeats periodically from plants, forms reflection bands in the spectrum of light passing through the structure. With an infinite crystal, such frequency ranges may form photonic band gaps. However, defects in the structure, spatial limits and dissipation lead to appearance of local modes in the form of spectral lines of finite width. The corresponding concentrating of intrinsic energy forms a secondary photonic structure consisting not of atoms but of photons. That's why they have unique optical properties.

The aim of this research was to study optical properties of epicuticular waxes of blue spruce and wheat. Their structures were to the fullest extent possible studied in [21–23]. A distinctive feature revealed is the visible discoloration caused by the structure of wax. Spruce acquires a blue color while wheat becomes blue-grey. An elementary wax unit, a tube sized 1-4 microns with a diameter of about 150 nm was discovered as part of the study.

2. Materials and microscopy

2.1. Wax isolation

As the material for the research, fresh needles of half-mature blue spruce (P. pungens) growing in natural environment and leaves of blue-grey wheat were collected. Only those needles and leaves were selected where blue tint along the whole surface was clearly visible, indicating the integrity of epicuticular wax.

In most cases, organic substances or solutions are used to separate the wax layer. These methods may complicate the quantitative spectral measurements due to some drawbacks such as capturing too large area, contaminating the material by the agents used, etc. Using sugar solution [21] is regarded as one of the best methods for such studies. The syrup penetrates the structure and upon drying, the sugar begins to crystallize. This makes the smallest formations, even individual nanotubes, snapp off. However, sugar still influences the results of optical measurements. The authors who proposed this method note that it is not easy to remove even after repeated rinsing with water. The use of organic solvents leads to formation of new chemical compounds and decomposition of the internal wax structure. In our opinion, the best technique is to use distilled water. This inert pure material penetrates deeply into the structure under the action of capillary forces and can be easily removed while vacuum drying.

The samples were placed in a vessel filled with distilled water for at least 5 hours. Then the water was freezed. When the water turns into ice it expands and wax plates come off. After thawing, the plates floated to the surface and were collected and then placed on substrates. The plates float to the surface due to the fact that their bulk density is less than the density of water and their energy of interaction with water is less than the energy of interaction with both metal and quartz substrates, so they stick to the latter.

Three types of substrates were used: quartz for optical studies; metal for high resolution electron microscopy; glass with an electrically conductive Ito-coating was used for the control group to conduct both optical and electronic research methods on the same sample.

2.2. SEM microscopy

Structural and morphological studies of the wax layer were performed by scanning electron microscopy using a Hitachi SU3500 microscope (accelerating voltage 10 kV, W-cathode) and a

high resolution scanning electron microscope Hitachi S-5500 (accelerating voltage 30 kV, field emission cathode).
The absence of chemical and solvent influence let us assume that we obtained minimally distorted samples for electron microscopy.
Sufficiently low accelerating voltage and beam current do not cause melting of the substance while a smooth substrate does not introduce geometric distortions. Fig. 1 obtained from the needles surface indicates the tubular structure of wax coating. The external diameter of the tubes is estimated to be 150 nm and 3-5 microns in length. The in-depth distance between nanotubes varies from 0 to 300 nm.

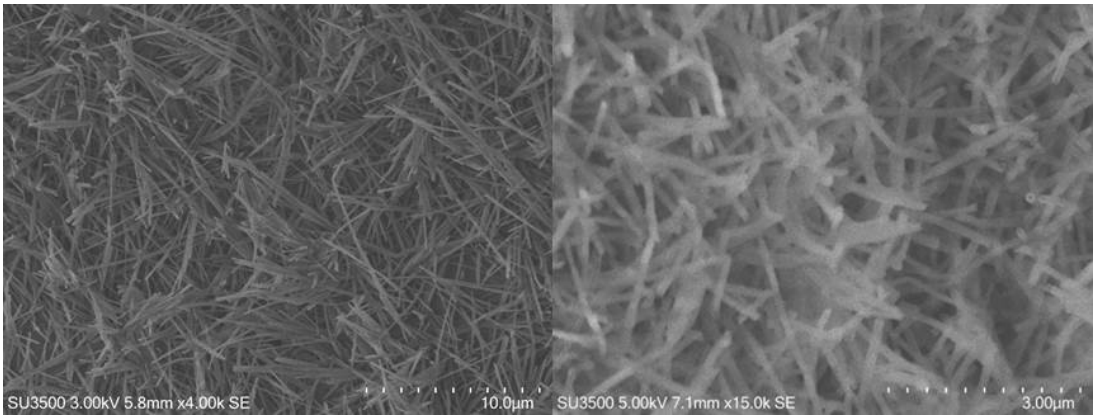

Figure 1. Photographs of wheat (Left) and blue spruce (Right) obtained with a scanning electron microscope.

3. Calculations

The number of research on the study of photonic crystals (PC) with high dielectric contrast and defects has been constantly growing with discovering of their new interesting features [24 - 30]. Classification of defects and their influence on the spectra of traditional PC structures with a wide band gap are described in [24].
In this research we developed two one-dimensional models based on open and sealed nanotubes located horizontally on each other (Fig. 2) considering vertical incidence of light. The first and last layers, the distance between the tubes and the inner space of the tubes are filled with air which refractive index equals to 1. Fig. 2 presents the mathematical model of a PC.

In this paper, normal incidence of light in a nonmagnetic medium ($\mu = 1$) was considered. The medium consists of layers of thickness LN with a refractive index nN. A plane electromagnetic wave propagates along the Oz axis. Waves amplitudes (A and B) going in the forward and back directions along the optical axis in the previous layer depend on the same values in the current layer [31]:

$$A_{N-1} = \frac{1}{2}((1 + \frac{n_N}{n_{N-1}})A_N e^{-i\frac{\omega}{c}n_N L_N} + (1 - \frac{n_N}{n_{N-1}})B_N e^{i\frac{\omega}{c}n_N L_N} +) \quad (1)$$

$$B_{N-1} = \frac{1}{2}((1 - \frac{n_N}{n_{N-1}})A_N e^{-i\frac{\omega}{c}n_N L_N} + (1 + \frac{n_N}{n_{N-1}})B_N e^{i\frac{\omega}{c}n_N L_N} +) \quad (2)$$

$$E(z, N) = A_N e^{-i\frac{\omega}{c}n_N L_N} + B_N e^{i\frac{\omega}{c}n_N L_N} \quad (3)$$

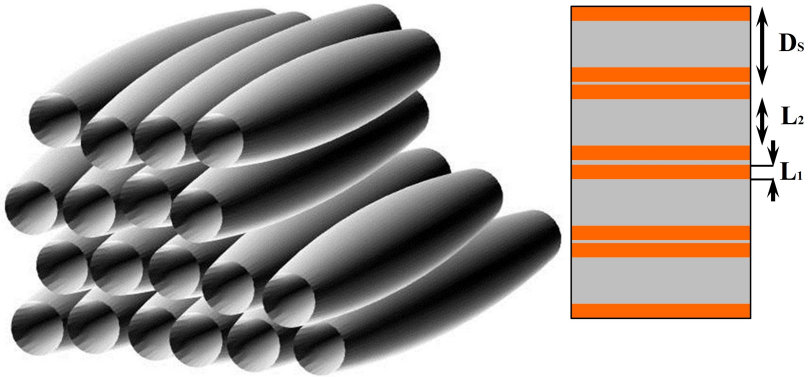

Figure 2. Model of tubules organized in rows (left). Estimated PC with parameters Ds = 140nm, L1 = 30nm, L2 = 80nm, N1 = 1.46, N2 = 1 (right).

$$H(z,N) = i\frac{\omega}{c} n_N (A_N e^{-i\frac{\omega}{c} n_N L_N} - B_N e^{i\frac{\omega}{c} n_N L_N}) \tag{4}$$

where N is layer number, E and H show distribution of electric and magnetic fields in the layer, $\omega = 2\pi v\chi$, χ is the scaling factor, χLN is linear size of the layer, v is frequency, c is the speed of light in vacuum. Keeping in mind that there is only an outgoing wave at the exit from the structure (Aout = 1; Bout = 0) and having made numerical calculations, we can get an array of relative values of the amplitudes in each of the PC layers. Thus, it is possible to find the distribution of electromagnetic field in the layered structure and its transmission spectrum. The transmittance coefficient kT [32, 33] (a precondition: refractive indices of the media before and after the sample are the same):

$$k_T = |A_0|^{-2} \tag{5}$$

A theoretical description of crystals photonic states density and its relationship with electromagnetic energy are described in detail in [34–37].
In [37], formula determining density of eigenmodes was proposed:

$$\rho_\omega = \frac{\frac{1}{2L_\Sigma}\int_0^{L_\Sigma}[\epsilon(\omega)|E_\omega|^2 + \frac{c^2}{\omega^2}|\frac{\partial E_\omega}{\partial z}|^2]\partial z}{c|E_\omega^I|^2} \tag{6}$$

where Eω is the amplitude of electromagnetic field electric component, E Iω is amplitude of incident wave, $\epsilon\omega$(z) is permittivity of the coordinate, Lσ is total thickness of the structure.
Considering PC models and the calculations described above, transmission spectra were obtained for a structure with hollow nanotubes and a structure with sealed nanotubes (Fig. 3).

Transmission spectrum let us obtain corresponding spectra of density of photon states (Fig.4).

4. Fluorescence

According to [38], density of photon states is directly proportional to fluorescence spectra. Fig. 5 presents fluorescence graphs obtained from isolated wax layers of blue spruce and blue-grey wheat.

Figures 4 and 5 show that the graphs of density of photon states and fluorescence graph are in complete agreement, which testifies convergence of the calculation.
Difference in transmission spectra between structures consisting of hollow (Fig. 3, top) and filled

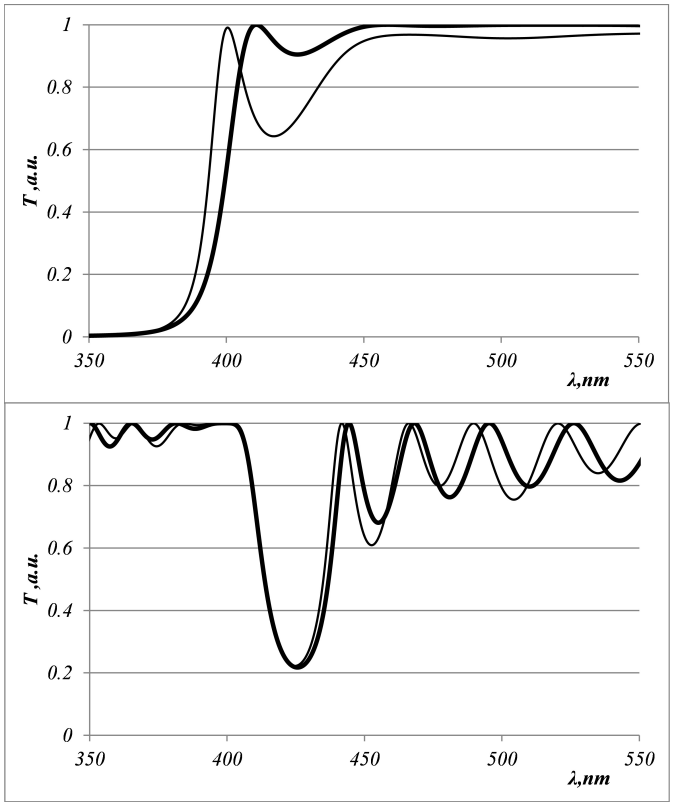

Figure 3. Transmission spectrum for a structure with hollow nanotubes at the top, transmission spectrum for a structure with filled nanotubes at the bottom. Thick line - Wax structure, Thin line - Wax structure with a defect.

(Fig. 3, bottom) nanotubes is caused by differences in structure of the two wax types. The top picture (Fig. 3) presents the structure of blue spruce wax. The one at the bottom shows the structure of wheat wax.

These structures also show some differences in fluorescence spectra (Fig. 5): the fluorescence peak is close to its border with ultraviolet (Fig.5, top), while for wheat (Fig. 5, bottom) it is closer to the green area.

It is notable that the defects in these structures influence the density of photon states. For instance, the structure consisting of hollow tubes, where a filled tube was used as a defect, presents higher values of photon states density (Fig. 4).

5. Conclusion

The morphological and optical characteristics of wax layers in blue spruce and blue wheat are studied. In both cases, nanotubes are the elemental structural unit. A large number of tubes in wheat are closed, while in blue spruce they are hollow. Modeling of the transmission spectra and the density of photon states of one-dimensional photonic crystals showed that their spectra are different, but a characteristic feature is that, under the influence of ultraviolet radiation, intense fluorescence appears in the visible area corresponding to the peaks of the density of photon states.

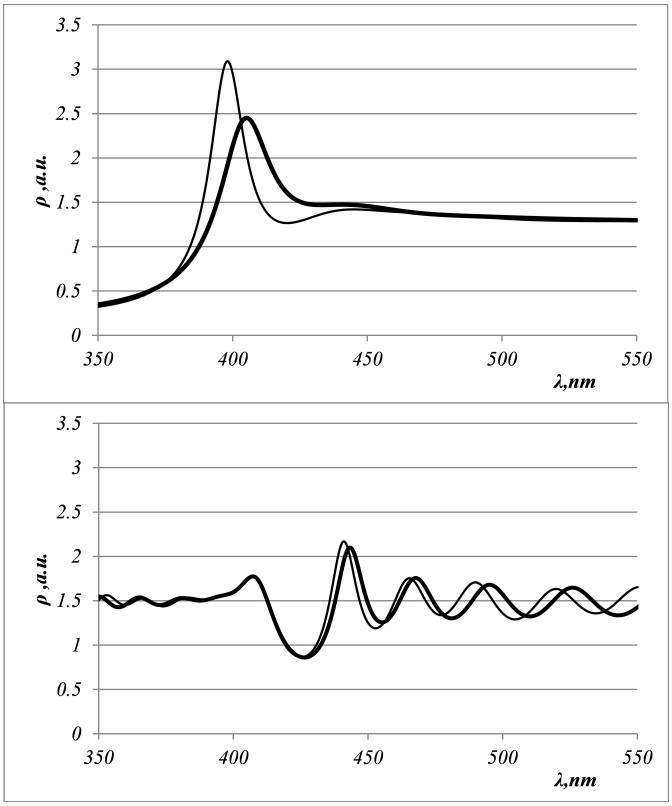

Figure 4. Density spectrum of photon states for a structure with hollow nanotubes at the top, density spectrum of photon states for a structure with filled nanotubes at the bottom. Thick line - Wax structure, Thin line - Wax structure with a defect.

6. Acknowledgments

The studies were performed on the equipment of the collective use center of the FRC KSC of the SB RAS.

7. References

[1] Weaver, J.M. Cuticular wax variants in a population of switchgrass (Panicum virgatum L.) / J.M. Weaver, G. Lohrey, P. Tomasi, J. M. Dyer, M. A. Jenks, K. A. Feldmann // Industrial Crops and Products. – 2018. – Vol. 117. – P. 310-316.
[2] Reicosky, D.A. Physiological Effects of Surface Waxes: I. Light Reflectance for Glaucous and Nonglacous Picea pungens / D.A. Reicosky, J.M. Hanover // Plant Physiol. – 1978. – Vol. 62. – P. 101-104.
[3] Harrington, C.A. Morphology and accumulation of epicuticular wax on needles of Douglas-fir / C.A. Harrington, W.C. Carlson // Northwest Science. – 2016. – Vol. 89(4). – P. 401-408.
[4] Dragota, S. Comparative study on epicuticular leaf waxes of Araucaria araucana, Agathis robusta and Wollemia nobilis / S. Dragota, M. Riederer // Australian Journal of Botany. – 2008. – Vol. 56(8). – P. 644-650.
[5] Guo, J. Cuticular Wax Accumulation Is Associated with Drought Tolerance in Wheat Near-Isogenic Lines / J. Guo, W. Xu, X. Yu, H. Shen, H. Li, D. Cheng, A. Liu, J. Liu, C. Liu, S. Zhao, J. Song // Front. Plant Sci. – 2016. – Vol. 7(1809). – P. 10.
[6] Bi, H. The impact of drought on wheat leaf cuticle properties / H. Bi, N. Kovalchuk, P. Langridge, P.J. Tricker, S. Lopato, N. Borisjuk // BMC Plant Biology. – 2017. – Vol. 17(85). – P. 1-13.

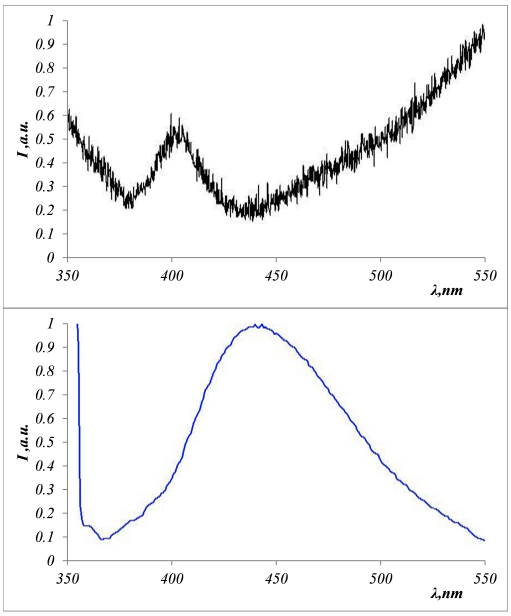

Figure 5. Fluorescence spectrum for a structure with hollow nanotubes at the top, fluorescence spectrum for a structure with filled nanotubes at the bottom.

[7] Koch, K. Structural analysis of wheat wax: from the molecular level to three dimensional crystals / K. Koch, W. Barthlott, S. Koch, A. Hommes, K. Wandelt, W. Mamdouh, S. De-Feyter, P. Broekmann // Planta. – 2005. – Vol. 223. – P. 258-270.
[8] Bianchi, G. Plant waxes. In Waxes: Chemistry, molecular biology and functions // The Oily Press, 1995. – P. 175-222.
[9] Barthlott, W. Classification and terminology of plant epicuticular waxes / W. Barthlott, C. Neinhuis, D. Cutler, F. Ditsch, I. Meusel, I. Theisen, H. Wilhelmi // J. Bot. Linnean Soc. – 1998. – Vol. 126. – P. 237-260.
[10] Barthlott, W. Scanning electron microscopy of the epidermal surface in plants. Scanning electron microscopy in taxonomy and functional morphology // Syst.Assoc. Spec. – 2001. – Vol. 41. – P. 69-94.
[11] Walton, T.J. Waxes, cutin and suberin – London: Academic, 1990. – P. 105-158.
[12] Kunst, L. Biosynthesis and secretion of plant cuticular wax / L. Kunst, A.S. Samuels // Prog. in Lipid Res. – 2003. – Vol. 42. – P. 51-80.
[13] Koch, K. Chemistry and Crystal Growth of Plant Wax Tubules of Lotus (Nelumbo nucifera) and Nasturtium (Tropaeolum majus) Leaves on Technical Substrates / K.A. Koch, A. Dommisse, W. Barthlott // Crystal growth and design. – 2006. – Vol. 6(11). – P. 2571-2578.
[14] Dora, S.K. Kinetics of solvent supported tubule formation of Lotus (Nelumbo nucifera) wax on highly oriented pyrolytic graphite (HOPG) investigated by atomic force microscopy / S.K. Dora, K. Koch, W. Barthlott, K. Wandelt // Beilstein J. Nanotechnol. – 2018. – Vol. 9. – P. 468-481.
[15] Dora, S.K. Real Time Recrystallization Study of 1, 2 Dodecanediol on Highly Oriented Pyrolytic Graphite (HOPG) by Tapping Mode Atomic Force Microscopy // World Journal of Nano Science and Engineering. – 2007. – Vol. 7. – P. 1-15.
[16] Dora, S.K. Recrystallization of tubules from natural lotus (Nelumbo nucifera) wax on a Au(111) surface / S.K. Dora, K. Wandelt // Beilstein J. Nanotechnol. – 2011. – Vol. 2. – P. 261-267.
[17] Poinern, E. Superhydrophobic nature of nanostructures on an indigenous Australian eucalyptus plant and its potential application / E. Poinern, X.T. Le, D. Fawcett / Nanotechnology, Sci. and App. – 2011. – Vol. 4. – P. 113-121.
[18] Lee, D. Nature's Palette: The Science of Plant Color – Chicago: University of Chicago Press, 2010. – 432 p.
[19] Vignolini, S. Analysing photonic structures in plants / S. Vignolini, E. Moyroud, B.J. Glover, U. Steiner // Journal R. Soc. interface. – 2013. – Vol. 10(87). – P. 1-9.

[20] Thomas, K.R. Function of blue iridescence in tropical understorey plants / K.R. Thomas, M. Kolle, H.M. Whitney, B.J. Glover, U. Steiner // J. R. Soc. Interface. – 2010. – Vol. 7(53). – P. 1699-1707.
[21] Ensikat, H.J. Direct access to plant epicuticular wax crystals by a new mechanical isolation method / H.J. Ensikat, C. Neinhuis, W. Barthlott // Int. J. Plant Sci. – 2000. – Vol. 161(1). – P. 143-148.
[22] Ensikat, H.J. Crystallinity of plant epicuticular waxes: electron and X-ray diffraction studies / H.J. Ensikat, M. Boese, W. Mader, W. Barthlott, K. Koch // Chem. and Phys. of Lipids. – 2006. – Vol. 144. – P. 45-59.
[23] Bukhanov, E.R. The effect of the structure on the optical properties of epicular blue spruce wax (Picea pungens) / E.R. Bukhanov, A.V. Shabanov, M.N. Krakhalev, M.N. Volochaev, Yu.L. Gurevich // Memoirs of the Faculty of Physics. – 2019. – Vol. 5. – P. 1950502-1-7.
[24] Eliseeva, S.V. Field and spectra of one-dimensional photonic crystal with inversion type defect / S.V. Eliseeva, V.A. Ostatochnicov, D.I. Sementsov // Computer Optics. – 2012. – Vol. 36(1). – P. 14-20.
[25] Doskolovich, L.L. Spatial differentiation of optical beams using phase-shifted Bragg grating / L.L. Doskolovich, D.A. Bykov, E.A. Bezus, V.A. Soifer // Opt. Lett. – 2014. – Vol. 39(5). – P. 1278-1281.
[26] Bykov, D.A. Optical computation of the Laplace operator using phase-shifted Bragg grating / D.A. Bykov, L.L. Doskolovich, E.A. Bezus, V.A. Soifer // Optics Express. – 2014. – Vol. 22(21). – P. 25084-25092.
[27] Golovastikov, N.V. Spatial optical integrator based on phase-shifted Bragg gratings / N.V. Golovastikov, D.A. Bykov, L.L. Doskolovich, E.A. Bezus // Optics Communications. – 2015. – Vol. 338. – P. 457-460.
[28] Nasedkina, Y.F. Transformation of a Gaussian pulse when interacting with a one-dimensional photonic crystal with an inversion defect / Y.F. Nasedkina, S.V. Eliseeva, D.I. Sementsov // Photonics and Nanostructures – Fundamentals and Applications. – 2016. – Vol. 19. – P. 31-38.
[29] Dadoenkova, Yu.S. Reshaping of Gaussian light pulses transmitted through one-dimensional photonic crystals with two defect layers / Yu.S. Dadoenkova, N.N. Dadoenkova, I.L. Lyubchanskii, D.I. Sementsov // Applied Optics. – 2016. – Vol. 55. – P. 3764-3770.
[30] Abram, R.A. A study of a phase formalism for calculating the cumulative density of states of one-dimensional photonic crystals / R.A. Abram, A.A. Greshnov, S. Brand, M.A. Kaliteevski // Journal of Modern Optics. – 2017. – Vol. 64(15). – P. 1501-1509.
[31] Shabanov, A.V. Investigation of the electromagnetic field in one-dimensional photonic crystals with defects / A.V. Shabanov, M.A. Korshunov, E.R. Bukhanov // Computer Optics. – 2017. – Vol. 41(5). – P. 680-686. DOI: 10.18287/2412-6179-2017-41-5-680-686.
[32] Shabanov, A.V. Features of the amplification of the electromagnetic field and the density of states of photonic crystal structures in plants / A.V. Shabanov, M.A. Korshunov, E.R. Bukhanov // Computer Optics. — 2019. — Vol. 43(2). – P. 231-237. DOI: 10.18287/2412-6179-2019-43-2-231-237.
[33] Shabanov, V.F. Optics of real photonic crystals [In Russian]. / V.F. Shabanov, S.Ya. Vetrov, A.V. Shabanov – Novosibirsk: Izdatelstvo SB RAS Publisher, 2005. – 209 p.
[34] Vats, N. Theory of fluorescence in photonic crystals / N. Vats, S. John, K. Busch // Physical Review A. – 2002. – Vol. 65. – P. 43808.
[35] Schmidtkea, J. Fluorescence of a dye-doped cholesteric liquid crystal film in the region of the stop band: theory and experiment / J. Schmidtkea, W. Stille // The European Physical Journal B. – 2003. – Vol. 31. – P. 179-194.
[36] D'Aguanno, G. Density of modes and tunneling times in finite one-dimensional photonic crystals: A comprehensive analysis / G. D'Aguanno, N. Mattiucci, M. Scalora, M.J. Bloemer, A.M. Zheltikov // Physical Review E. – 2004. – Vol. 70. – 16612.
[37] D'Aguanno, G. Photonic band edge effects in finite structures and applications to x2 interactions / G. D'Aguanno, M. Centini, M. Scalora, C. Sibilia, Y. Dumeige, P. Vidakovic, J.A. Levenson, M.J. Bloemer, C.M. Bowden, J.W. Haus, M. Bertolotti // Physical Review E. – 2001. – Vol. 64. – P. 16609.
[38] Dolganov, P.V. Spectral features of cholesteric luminescence photonic crystal // JETP Letters. – 2017. – Vol. 105(10). – P. 616-620.